CHAPTER 6

EFFECT OF TEMPERATURE ON BRITTLE-DUCTILE TRANSITION AND CRITICAL DEPTH OF CUT FOR 45S5 BIOGLASS

This chapter describes the brittle-ductile transition and critical depth of cut for 45S5 bioglass at different temperatures. The specimen temperature is kept at room temperature (27 °C), 100 °C, 250 °C, 400 °C, 550 °C and 700 °C for the experiments. The modified bifano model is proposed to calculate the critical depth of cut at different temperatures. The experimental setup explaining the nature of tests to study the effect of temperature on brittle-ductile transition and critical depth of cut for 45S5 bioglass has already been discussed in section 3.7.

6.1 Operating parameters

While performing the elevated temperature scratch tests, the specimen temperature is kept at room temperature (27 °C), 100 °C, 250 °C, 400 °C, 550 °C and 700 °C for the experiments described. The heat controller of the multipurpose portable heating setup has been used to regulate and monitor the projected temperature of the sample surface. It has also been considered that there should not be a sharp increase in temperature in the samples because this could create thermal strains to induce cracks. As a result, the sample is heated at a rate of not more than 10 °C per min. After that, the steady-state temperature has been considered for at least 15 min to ensure that the sample does not continue to heat up. During the experiments, ramp loading was chosen with a starting load of 10 N and a loading rate of 2 N/mm. The length of the scratch stroke was left at 5 mm. The final load after the 5 mm scratch will therefore be 20 N. The scratch speed is kept at 1.0 mm/s consistently. The offset between two adjacent scratches measured 0.5 mm. Table 6.1 displays the elucidated scratch conditions. There are six scratches made at different

temperatures while other parameters are kept constant. Here, every scratch condition was repeated 3 times.

Table 6.1:Projected scratch conditions

Temp. (°C)	Load Type	Load Range (N)	Start Load (N)	End Load (N)	Loading Rate (N/mm)	Stroke (mm)	Scratch Speed (mm/s)	Scratch Offset (mm)
27 100 250 400 550 700	Ramp	0-20	10	20	2	5	1	0.5

6.2 Experimental procedure

Since the ramp load is chosen for the scratch, the depth of penetration, in the beginning, will be less and it will continuously increase with further movement of the scratch probe. A typical scratch with ramp load consists of ploughing, ductile and brittle zone if the starting load is zero during a scratch test with ramp loading. Experimentally, the starting load and loading rate are selected so that the scratch starts in ductile mode of scratch and

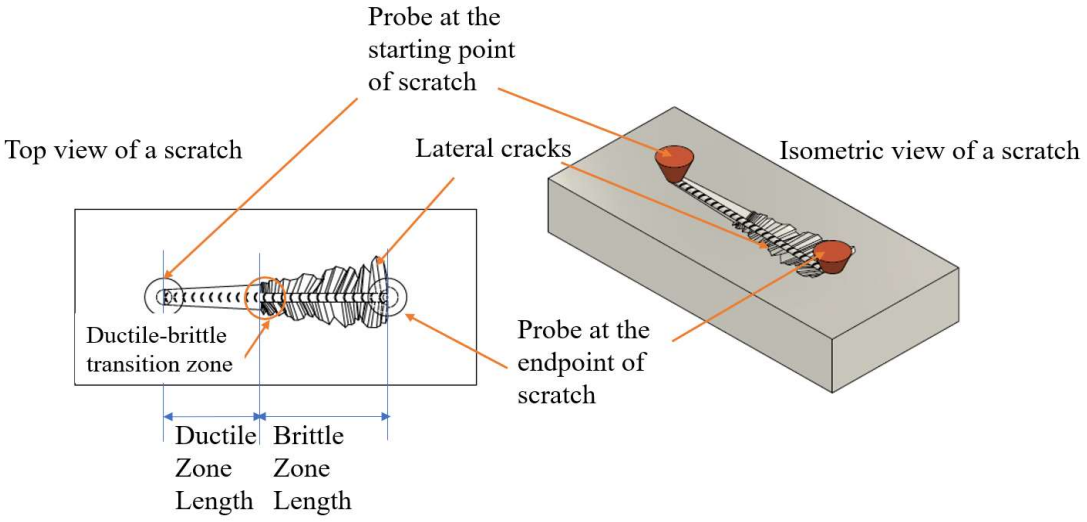

Figure 6.1: Illustration of a typical scratch with ramp loading

ends in brittle mode. Figure 6.1 shows the CAD model illustration of a typical scratch with ramp loading. It shows the start and end position of the probe as well as the transformation of ductile to brittle mode of scratch. The top view (Figure 6.1) of the scratch shows the ductile-brittle transition zone as well as the ductile zone length and brittle zone length of the scratch. The ductile-brittle transition zone represents the limiting condition for material to undergo the brittle fracture. Therefore, our focus is to obtain the depth of penetration at the ductile-brittle transition zone. This depth of penetration represents the maximum depth of cut for a material to experience a ductile failure. Therefore, the depth of penetration at the ductile-brittle transition represents the critical depth of cut.

Figure 6.2 shows a typical example of a parametric evaluation of a scratch at 27 °C. For taking the optical images of the scratches have been taken using an optical microscope

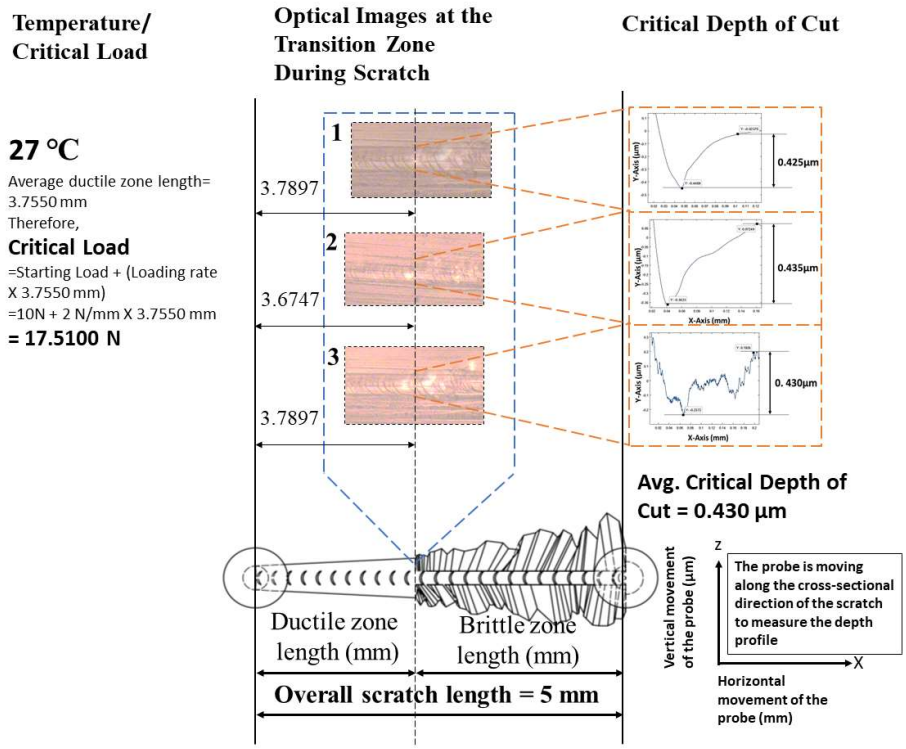

Figure 6.2: Parametric evaluation of a scratch at 27 °C

with a 500X imaging magnification. Here, the optical images have been taken at the ductile-brittle transition zone and the ductile zone length is measured. This length multiplied by the loading rate (2 N/mm) represents the brittle fracture starting load (critical load). Subsequently, the cross-sectional profile of the scratch is measured with the help of Mitutoyo Surftest (SV-2100). While measuring the cross-sectional profile, the probe of the machine moved on the sample surface at 90° to the scratch direction. This cross-sectional profile measurement has been taken between the end of the ductile zone and the start of the brittle zone as shown in Figure 6.2. The measured profile is further analyzed and the maximum depth from the sample surface is taken. Since the maximum depth of cut is taken at the ductile-brittle transition zone, it represents the critical depth of cut (DOC) for a particular scratch condition.

Apart from the scratch tests, the elevated temperature microhardness tests are also performed using a Vickers microhardness tester and a portable heating setup. To perform elucidated experiments, the samples assembled on the portable heating setup were placed at the vice of the micro scratch tester. The experimentation was performed at 27 °C, 100 °C, 250 °C, 400 °C, and 550°C. It has also been considered that there should not be a sharp increase in temperature in the samples because this could create thermal strains to induce cracks in samples. As a result, the sample is heated at a rate of no more than 10 °C per min. After that, the steady-state temperature has been considered for at least 15 min to ensure that the sample does not continue to heat up. During the experiments, 50 g loading is chosen with a 500X imaging magnification. Furthermore, the average crack length (C_t) is determined with 100 g loading, 500 X imaging magnification and the dwell time of loading is kept at 10 s. All these evaluations are used to develop a model for the critical depth of cut for 45S5 bioglass.

6.3 Results and discussion

The parametric evaluation of scratch test at 27 ℃, 100 ℃, 250 ℃, 400 ℃, 550 ℃, and 700 ℃ is shown in Figure 6.2 to Figure 6.7 respectively. The ductile zone length is measured for every set of scratch tests. Based on the ductile zone length, the critical load is calculated for the temperatures 27 °C, 100 °C, 250 °C, 400 °C, 550 °C, and 700 °C. The cross-section profile evaluation of scratches gives the critical depth of cut for the corresponding temperatures. The optical images of the ductile-brittle transition zone, profile for critical depth of cut, and ductile zone length at every temperature are shown in every parametric evaluation of scratch tests.

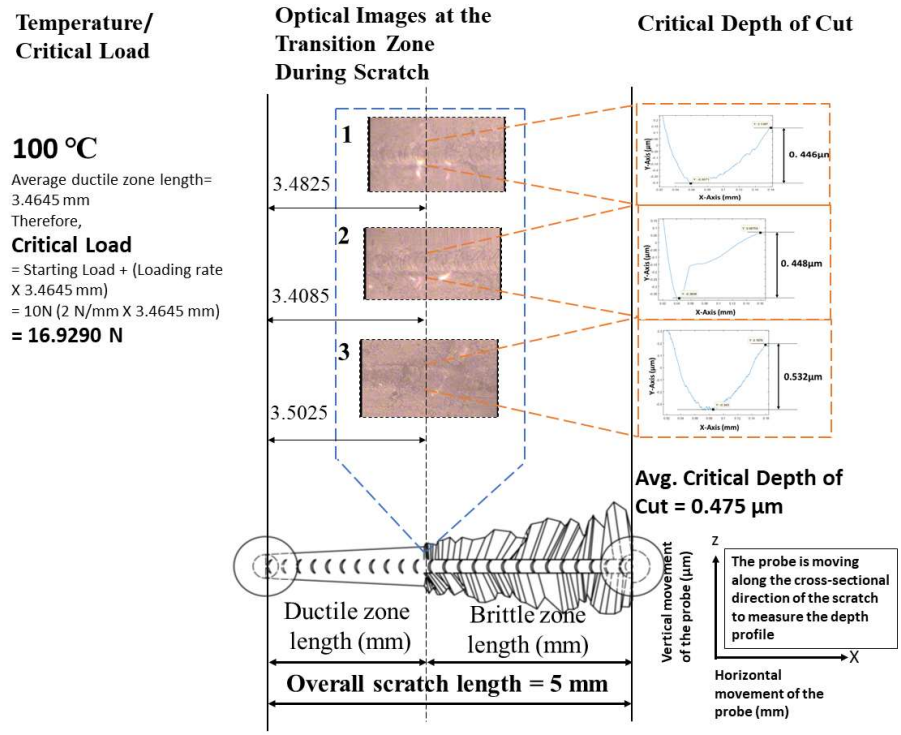

Figure 6.3: Parametric evaluation of a scratch at 100 ℃

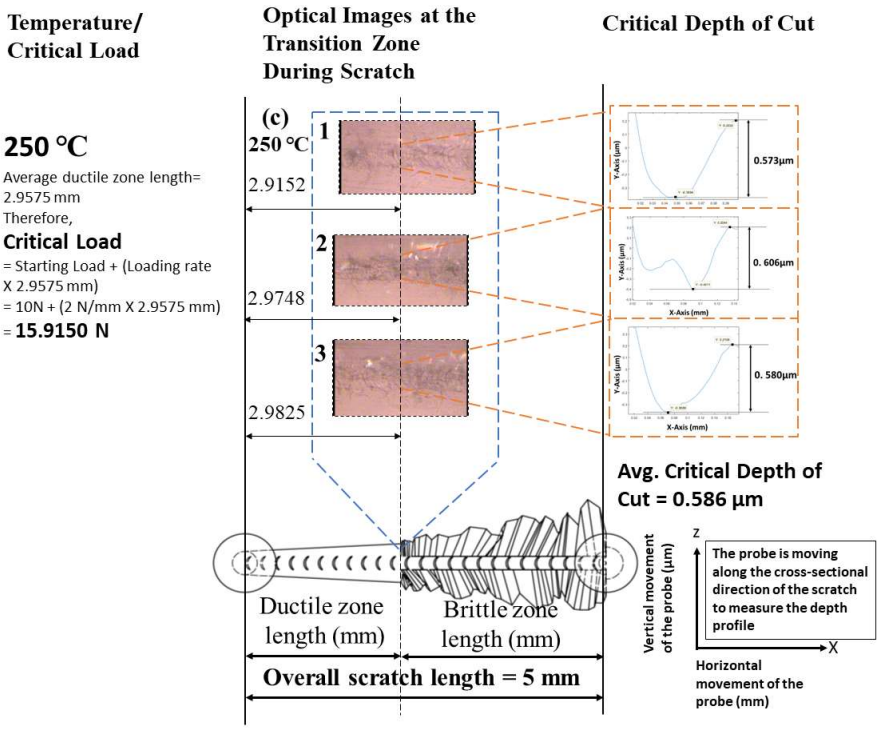

Figure 6.4: Parametric evaluation of a scratch at 250 °C

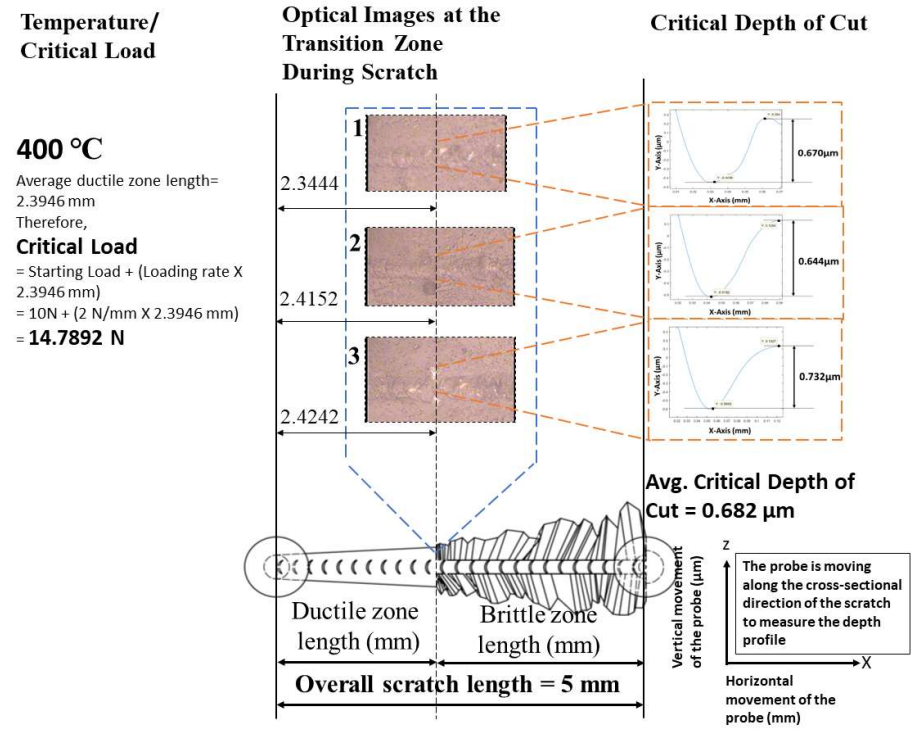

Figure 6.5: Parametric evaluation of a scratch at 400 °C

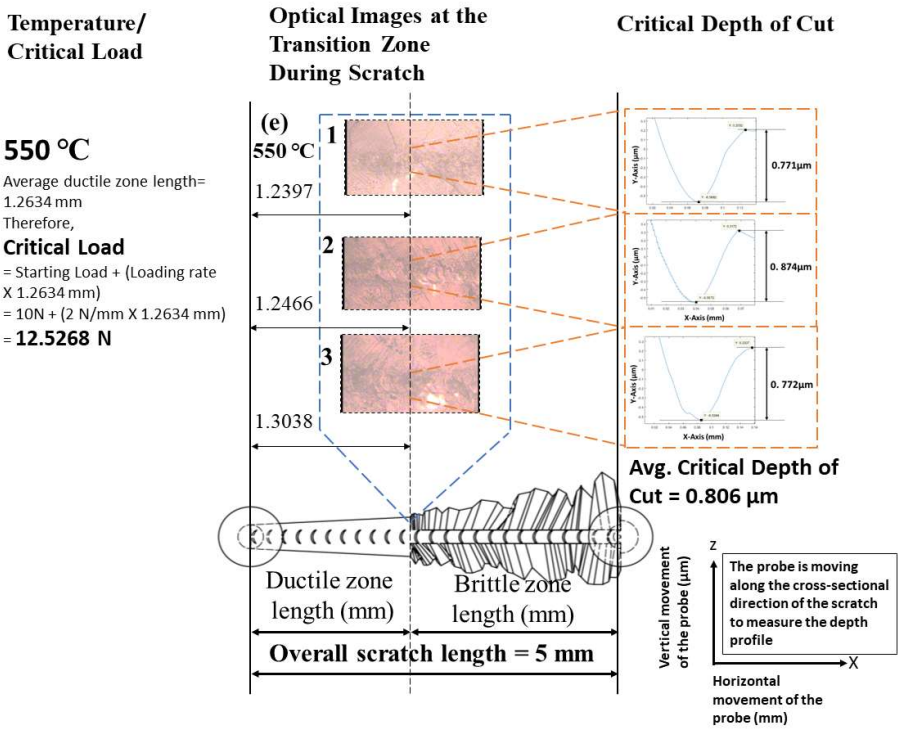

Figure 6.6: Parametric evaluation of a scratch at 550 °C

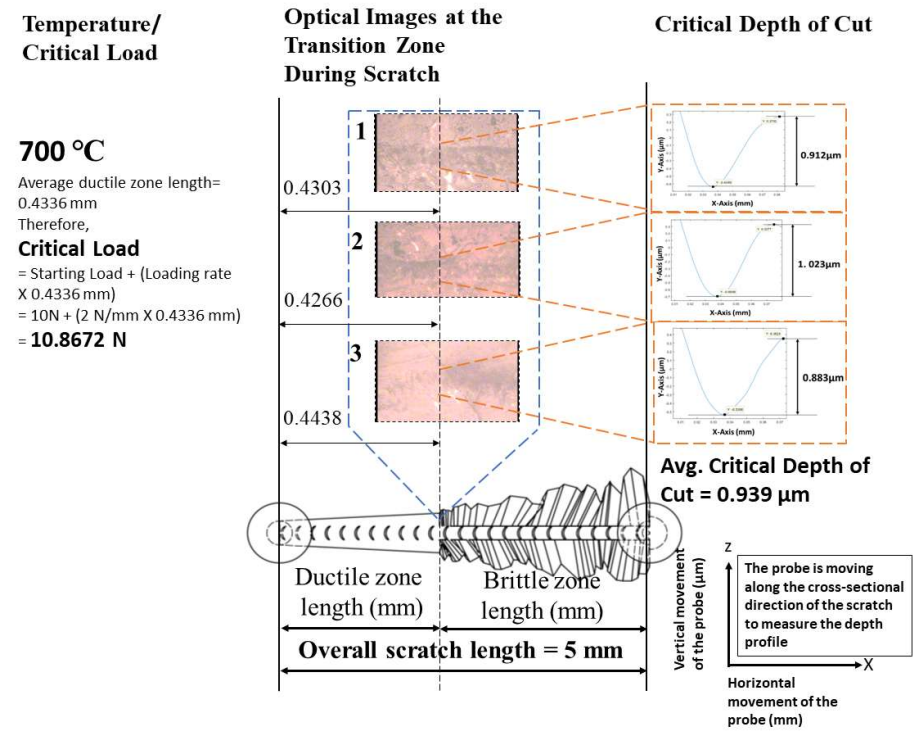

Figure 6.7: Parametric evaluation of a scratch at 700 °C

Performing the microhardness test at elevated temperatures gives the hardness value of 45S5 bioglass at temperatures 27 °C, 100 °C, 250 °C, 400 °C, and 550 °C. Table 6.2 shows the hardness values at different temperatures with 3 repetitions of each set. Subsequently, Table 6.3 shows the indentation images for hardness at different temperatures. While performing the scratch tests, the forces acting on the probe opposite to the scratch direction are termed traction force. The vertical load applied by the probe on the sample surface is termed a normal load. These forces are measured with the help of a load cell mounted on the micro scratch tester as discussed in section 3.7. The critical load is the measured normal load at the ductile-brittle transition. With the help of evaluations shown in Figures 6.2 to 6.7 and Table 6.2, different graphs are plotted as shown in Figure 6.8. While performing the elevated temperature scratch test, the normal and traction forces are recorded for each set of experiments. The traction forces for the temperature from 27 °C to 700 °C, are plotted against the scratch distance as shown in Figure 6.8(a).

Table 6.2: Evaluation of Average hardness at different temperatures

S. No.	**Temperature (°C)**	**Microhardness (HV)**			**Average hardness (HV)**
		(1)	(2)	(3)	
1	550	434.59	469.26	467.6	457.15
2	400	497.89	481.52	525.63	501.68
3	250	529.21	557.49	610.25	565.65
4	100	663.19	648.06	673.15	661.47
5	27	694.29	697.30	735.21	708.94

Table 6.3: Indentation images for hardness at different temperatures

Temperature (°C)	Indentation Image and Hardness (HV) Run-1	Run-2	Run-3	Avg. Hardness (HV)
550	 434.59	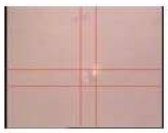 469.26	 467.6	457.15
400	 497.89	 481.52	 525.63	501.68
250	 529.21	 557.49	 610.25	565.65
100	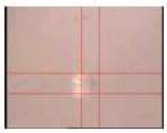 663.19	 648.06	 673.15	661.47
27	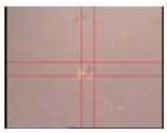 694.29	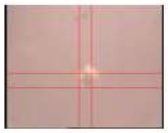 697.3	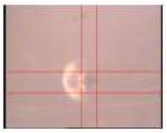 735.21	708.94

All traction plots at different temperatures are shown with different colours. It gives us a clear insight into the process that the traction forces are higher at lower temperatures. It implies that the probe needs less energy to produce a failure to the material in the lateral direction at high temperatures. Subsequently, the lower traction forces lead to better machinability of the material.

Figure 6.8(b) shows the graph between critical load and temperature. This graph indicates that the value of the critical load decreases with an increase in temperature. Therefore, it indicates that the higher temperature promotes the brittle fracture of material at a lower normal load. Apparently, Figure 6.8(c) shows the graph between the hardness and temperature of the material. The nature of the curve implies that there is a decrease in hardness with an increase in the temperature of the material and hardness values lie

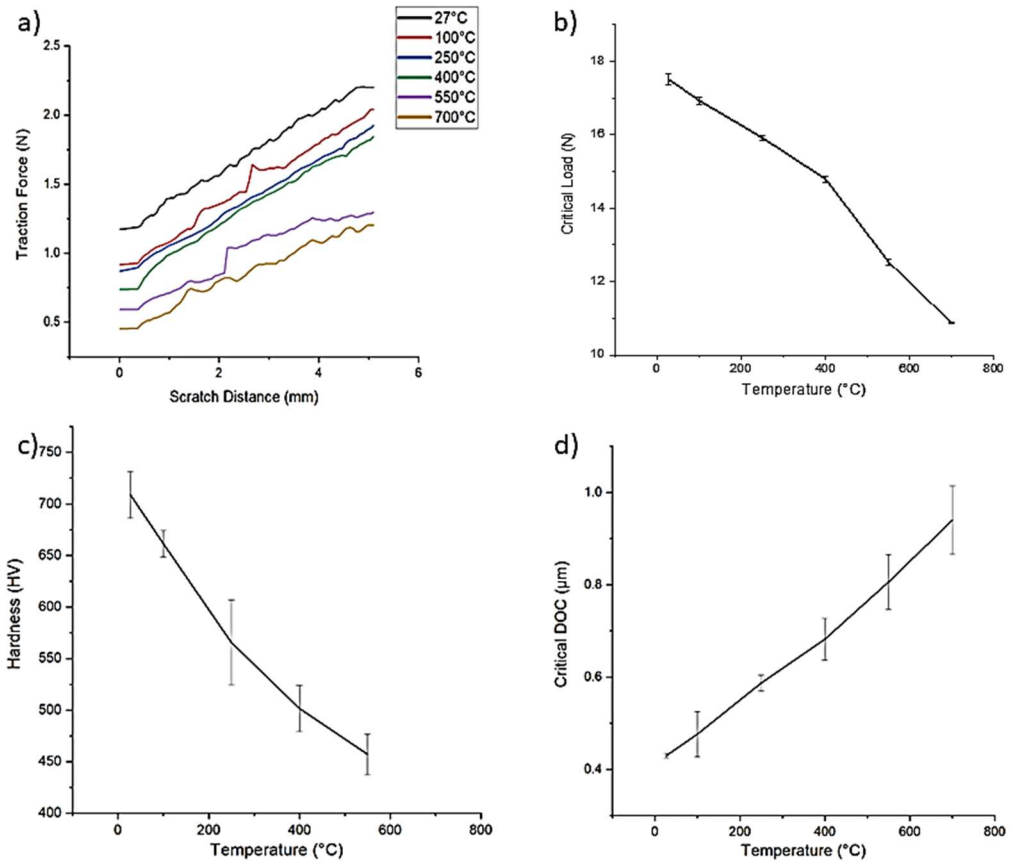

Figure 6.8: (a)Traction force (N) plot against the scratch distance (mm) at different temperatures (°C), (b) Critical load (N) vs temperatures plot (°C), (c) Hardness (HV) vs temperature plot (°C), and (d) Critical DOC (um) vs temperature (°C) plot

between 457.15 HV and 708.94 HV for the temperature range between 27 to 550 °C. Figure 6.8(d) shows the graph between critical DOC and temperature. Here, the nature of the curve shows that there is a significant increase in critical DOC with an increase in sample temperature for the temperature range between 27 to 700 °C.

Here, a decrease in hardness, decrease in critical load, and increase in critical depth of cut, are happening collectively with the rise in temperature of the sample. The reduction in hardness of the material allows the probe to create surface damage at a lower normal load. Subsequently, the penetration depth of the probe on the surface significantly increased because of thermal softening, which results in the higher critical DOC at higher temperatures. These collective outcomes tend to improve the machinability of the material at higher temperatures for 45S5 bioglass.

The method used to calculate fracture toughness (K_{IC}) was given as follows[10]:

$$K_{IC} = \alpha \left(\frac{E}{H}\right)^{\frac{1}{2}} \left(\frac{P}{C^{3/2}}\right) \tag{6.1}$$

where α=0.016, is an empirical constant depending on the geometry of the indenter, E is the elastic modulus, H is the hardness, C is the crack length and P is the peak indentation load.

When machining brittle materials, the change from a brittle to a ductile mode is defined in terms of the energy balance between the surface energy and the strain energy [11]. The critical indentation depth (d_c) for fracture initiation is given as follows [26]:

$$d_c = b \left(\frac{E}{H}\right) \left(\frac{K_{IC}}{H}\right)^2 \tag{6.2}$$

where b is a constant.

Bifano et al. established a correlation between the calculated critical depth of cut and the measured critical grinding infeed rate. From this correlation, the constant of proportionality for Equation (6.2) was estimated [11].

$$d_c = 0.15 \left(\frac{E}{H}\right) \left(\frac{K_{IC}}{H}\right)^2 \tag{6.3}$$

For the present study, the Equation (6.1) is re-written and the fracture toughness at different temperatures is given as,

$$K_{ICt} = \alpha \left(\frac{E_t}{H_t}\right)^{\frac{1}{2}} \left(\frac{P}{C_t^{3/2}}\right) \quad (6.4)$$

where, E_t is the elastic modulus, H_t is the hardness, and C_t is the crack length at a given temperature t during indentation.

The critical DOC at a given temperature t is,

$$d_{ct} = K_t \left(\frac{E_t}{H_t}\right) \left(\frac{K_{ICt}}{H_t}\right)^2 \quad (6.5)$$

where, K_t is proportionality constant at given temperature t. The elastic modulus of melt derived 45S5 bioglass is approximately 50-55 MPa [75]. This value of elastic modulus is very close to the elastic modulus of flint glass (F-689). Therefore, the elastic modulus (E_t), is taken from the high-temperature elastic modulus values of a flint glass (F-689) as given by Spinner [76]. These values are shown in Table 6.4 and the regression model for these values is given in Figure 6.9(a). The purpose of the hardness test was to achieve the elevated temperature harness curve for 45S5 bioglass. Figure 6.9(b) shows the curve for elevated temperature hardness. Therefore, the peak indentation load (P) was kept fixed at 0.1 Kg and the hardness test was performed at different temperatures. Hence, the same values are used for the calculation of the proportionality constant (K_t) as shown in Table 6.4. The Crack length (Ct) is calculated with the help of indentation tests at different temperatures. The average crack length (Ct) is determined with 100 g loading, 500 X imaging magnification and the dwell time of loading is kept at 10 seconds. Critical depth of cut (d_{ct}) every scratch condition is obtained from Figures 6.2 to 6.7. The regression model for crack length at elevated temperature is shown in Figure 6.9(c). With the help of the above-mentioned data, the fracture toughness at the corresponding temperature is calculated using Equation (6.4) as shown in Table 6.4. Further, the critical DOC values at corresponding temperatures are taken from Figure 6.8(d). These values are shown in Table 6.4. Using Equation (6.5), the values of the proportionality constant (K_t) have been

calculated and shown in Table 6.4. The regression model to predict the K_t is shown in Figure 6.9(d).

Table 6.4: Calculations for proportionality constant, K_t

S. No.	Temp.(T) (°C)	α	E_t (GPa)	H_t (HV)	P (Kg)	C_t (mm)	K_{ICt} (MPa/m^2)	d_{ct} (µm)	K_t
1	27	0.016	55.0	708.94	0.1	0.0113	3.75	0.43	0.19
2	100	0.016	54.0	661.47	0.1	0.0146	2.62	0.476	0.35
3	250	0.016	53.6	565.65	0.1	0.021	1.63	0.587	0.69
4	400	0.016	51.9	501.68	0.1	0.0294	1.03	0.682	1.47
5	550	0.016	48.9	457.15	0.1	0.0412	0.63	0.806	3.72

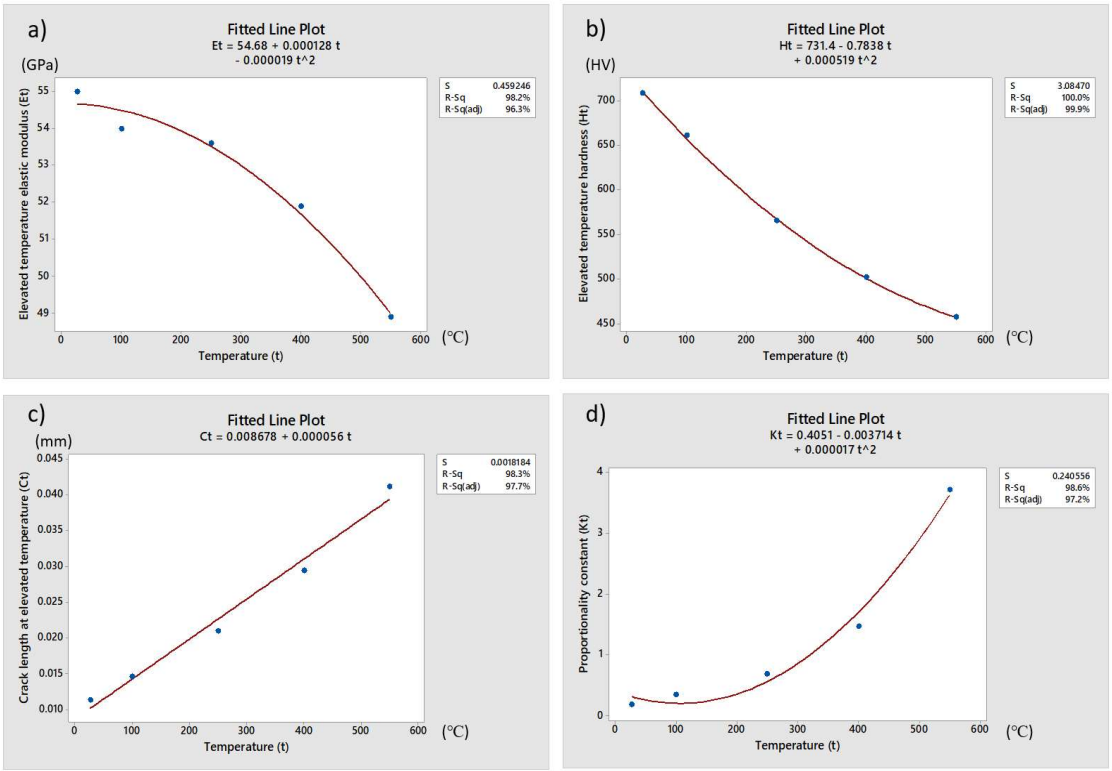

Figure 6.9: Regression model for; (a) Elevated temperature elastic modulus (Et), (b) Elevated temperature hardness (Ht), (c) Crack length at elevated temperature (Ct), and (d) Proportionality constant (Kt)

Since, the values of E_t, H_t, C_t, and K_t are dependent on temperature variation and their values are to be substituted in Equations (6.4) & (6.5). Therefore, the Equation (6.4) & (6.5) will be governed by the following supporting equations developed by the regression models;

$$E_t = 54.68 + 0.000128\,t - 0.000019t^2 \quad (6.6)$$

$$H_t = 731.4 - 0.7838t + 0.000519t^2 \quad (6.7)$$

$$C_t = 0.008678 + 0.000056t \quad (6.8)$$

$$K_t = 0.4051 - 0.003714t + 0.000017t^2 \quad (6.9)$$

Since the model is calibrated using temperature data ranging from 27℃- 550℃, the model is good for this temperature range only. Lower traction forces as a result of the increased temperature results in enhanced machinability for brittle materials at higher temperatures. Elevated temperature thus caused the material to have lower hardness as well as lower critical load during scratching. The conclusion is that higher temperatures generate ductile-brittle transmission at a relatively low normal load and result in higher critical DOC, which raises MRR. Through this research, it is more likely that samples of 45S5 bioglass and other ceramic materials will be easier to machine at high temperatures.

6.4 Summary

Six sets of scratches have been performed on 45S5 bioglass samples at scratch speed of 1 mm/s as well as sample temperatures 27 ℃, 100 ℃, 250℃, 400℃, 550℃ and 700 ℃. The ramp load of 10 - 20 N is applied to the sample with a scratch length of 5 mm. Five sets of hardness tests are also performed at sample temperatures 27 ℃, 100 ℃, 250℃, 400℃, and 550℃. The elevated temperature results in lower traction forces during the scratch test which indicates better machinability at higher temperatures for brittle materials. Subsequently, elevated temperature led to lower hardness as well as lower critical load during scratch on the material. Therefore, it has been conclusively established that greater temperatures cause ductile-brittle transmission at relatively lower normal load and produces higher critical DOC, which raises MRR. The fracture toughness (K_{ICt}) at temperature t is given in Equation (6.4). The elastic modulus (E_t), hardness (H_t) and crack length (C_t) is calculated from Equation (6.6), (6.7) and (6.8) respectively. Further, these values are used to calculate the critical DOC (d_{ct}) at temperature with the help of Equation (6.5) and the value of the proportionality constant at temperature t is given in Equation

(6.9). Therefore, Equation (6.5) represents the modified Bifano model for the determination of the critical depth of cut at elevated temperature for 45S5 bioglass. This work increases the likelihood that 45S5 bioglass and other ceramic samples will be more machinable at high temperatures.